CHAPTER 3

BIDENTATE [N,O]-DONOR SALICYLALDIMINE SCHIFF BASE LIGAND AND ITS MESOMORPHIC AND PHOTOLUMINESCENT TETRAHEDRAL d^{10}-METAL COMPLEXES

CHAPTER 3

BIDENTATE [N,O]-DONOR SALICYLALDIMINE SCHIFF BASE LIGAND AND ITS MESOMORPHIC AND PHOTOLUMINESCENT TETRAHEDRAL d^{10}-METAL COMPLEXES

3.1. Introduction

Materials that are photo-responsive and possess highly ordered fluid-phases are currently enjoying much interest for their applications such as OLEDs, information storage, sensors, lasers and enhanced contrast displays, etc.[1,2] Luminescence property of metal complexes coupled with the self-organizing ability of liquid crystals(LCs) offer a viable option to access multifunctional materials.[3,4] Amongst metals, lanthanides have widely been employed in synthesizing luminescent metallomesogens.[5,6] Luminescence of metallomesogens incorporating d-block metals such as palladium(II),[7,8] platinum(II),[9,10] iridium(III),[11,12] nickel(II),[13,14] rhenium(I),[15] gold(I),[16,17] silver(I),[17,18] zinc(II)[19,20] and copper(I)[21] have also attracted considerable interests. It is pertinent to mention here that complexes of zinc(II) and its congener cadmium(II) and mercury(II) display interesting fluorescent properties that originate from ligand-centred charge transfer or metal-centred luminescent levels providing access to newer functional materials.[22,23]

In addition to their manifold applications in the areas such as agriculture, drug design, polymers, catalysts and optoelectronics etc., [24-31] metal-salicylaldimines, currently have also earned a place of interest as liquid-crystalline materials.[32] As for salicylaldimines, the ease of synthesis as well as the flexibility of the co-ordination environment around the imine moiety render them a versatile class of ligands in co-ordination chemistry.[29] Salicylaldimine based metallomesogens has been accessed mostly with palladium(II),[33] copper(II),[34,35] oxovanadium(IV),[35,36] nickel(II),[36] iron(III),[37], manganese(III)[38] or lanthanides.[5,39] While examples of zinc are scarce,[40] those that incorporate cadmium and mercury ions appear to be virtually non-existent. Apart from a very early account of

mesomorphic cadmium alkanoates[41] or porphyrin as ligands,[42] only sporadic mention of cadmium based mesogens has been made in the literature. An unpublished reference to uncharacterized cadmium and mercury complexes of di-thiobenzoate with ill-defined phases was made in 1993.[43] Aquated cadmium ions $[Cd(H_2O)_4]^{2+}$, upon complexation with non-ionic oligo(ethylene oxide)surfactants, have been reported to form liquid crystalline phases.[44,45] Further, another interesting variety of complexes, tetrachlorometallates, $[MCl_4]^{2-}$ (M = Zn and Cd) with n-alkylpyridinium as counter-cation were reported to exhibit smectic mesomorphism.[46] Mesomorphic zinc complexes were previously reported to be either square planar or trigonal-bipyramidal.[47] Zinc metal ion usually prefers a tetrahedral geometry which often results in the loss of the mesomorphism.[20,48] Tetrahedral zinc complexes exhibiting mesomorphism have appeared only in the current decade and are limited to only a few examples,[20,40,49-52] and the ones that are both luminescent and liquid crystalline are rare. In fact there appears to be only a couple of instances in the literature of the latter type.[20,40,50,51] As against tetradentate 'salen' type ligands which enforce a planar geometry, bidentate ligands with long alkyl arm due to greater flexibility allow the metal ion to acquire thermodynamically stable tetrahedral geometry ensuring enhanced order in the molecular self-assembly.

Accordingly, in this chapter, we report synthesis of luminescent tetrahedral zinc(II), cadmium(II) and mercury(II) complexes of a new flexible one ring N-alkylated [N,O]-donor rod shaped salicylaldimine Schiff base ligand. The ligand is non-mesomorphic and lacks any fluorescence. Except the mercury(II) complex which decomposes before melting, zinc(II) and cadmium(II) complexes exhibit highly ordered mesophases.

3.2. Experimental

The general preparative route for the salicylaldimine ligand and its d^{10} metal complexes is presented in **Scheme 3.1**.

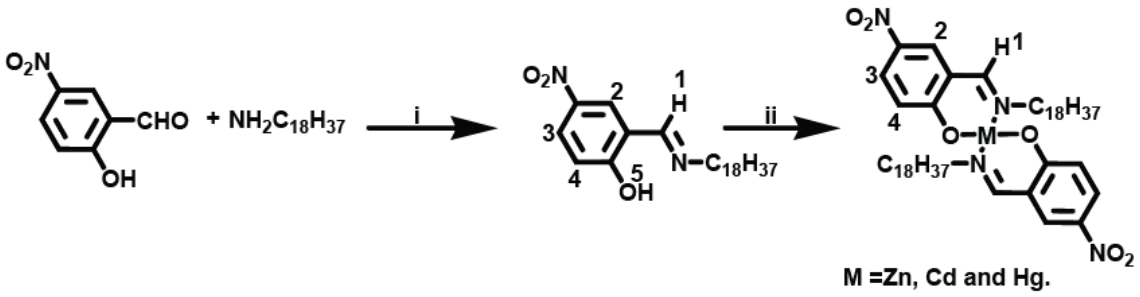

Scheme 3.1: i. Glacial acetic acid, methanol, reflux 3h, ii. $M(OAc)_2.nH_2O$ (M = Zn, Cd; n = 2 or Hg; n = 0), Methanol, stir, 2h.

3.2.1. Synthesis of ligand

Synthesis of 4-nitro-2-((octadecylimino)methyl)phenol, HL

A methanolic solution of 5-nitro salicylaldehyde (0.84g, 5 mmol) was added to a methanolic solution of octadecylamine (1.35g, 5 mmol). The solution mixture was heated under reflux with a few drop of acetic acid as catalyst for 3h to yield the yellow Schiff base. The compound was collected by filtration and re-crystallized from methanol.

Yield ~1.81g (82.49 %) Anal. Calc. (%) for $C_{25}H_{42}N_2O_3$ (418.63): C, 71.66; H, 10.04; N, 6.68. Found: C, 71.66; H, 10.06; N, 6.65%. FAB Mass: m/z = 418.3 (M^+-H). ^{1}H NMR (300 MHz, $CDCl_3$; Me_4Si at 25°C, ppm): δ = 15 (s, 1H; H^5), 8.31 (s, 1H; H^1), 8.23 (d, $^4J_{(H,H)}$ = 3.0 Hz, 1H; H^2), 8.19 (dd, $^3J_{(H,H)}$ = 6.0 Hz, $^4J_{(H,H)}$= 3.0 Hz, 1H; H^3), 6.90 (d, $^3J_{(H,H)}$ = 6.0 Hz, 1H; H^4), 3.66 (t, $^3J_{(H,H)}$ = 6.0 Hz, 2H; =N-CH_2), 0.88 (t, $^3J_{(H,H)}$ = 6.0 Hz, 3H; CH_3), 1.36 (m, -CH_2 of methylene proton in side chain). IR (ν_{max}, cm^{-1}, KBr): 3428 (ν_{OH}), 2917 ($\nu_{as(C-H)}$, CH_3), 2848 ($\nu_{s(C-H)}$, CH_3), 1672 ($\nu_{C=N}$), 1280 (ν_{C-O}).

3.2.2. Synthesis of zinc(II), cadmium(II) and mercury(II) complexes, [ML_2] (M = Zn, Cd, Hg)

General procedure:

In a separate reaction, to a methanolic solution of the ligand; **HL** (0.084g, 0.2mmol), methanolic solution of $Zn(OAc)_2.2H_2O$ (0.02 g, 0.1 mmol) or $Cd(OAc)_2.2H_2O$ (0.026 g, 0.1 mmol) or $Hg(OAc)_2$ (0.032 g, 0.1 mmol) was added. The mixture was stirred for 2h at

room temperature. A creamy white solid formed in each case was immediately filtered, washed with diethyl ether and re-crystallized from dichloromethane/methanol (1:1).

[ZnL_2]

Yield ~ 0.07g (70 %) Anal. Calc. (%) for $C_{50}H_{82}N_4O_6Zn$ (900.64): C, 66.62; H, 9.10; N, 6.22. Found: C, 66.63; H, 9.12; N, 6.20%. FAB Mass: m/z = 898.6 (M^+-H). ^{1}H NMR (400 MHz, $CDCl_3$; Me_4Si at 25°C, ppm): δ = 8.30 (s, 1H; H^1), 8.25(d, $^4J_{(H,H)}$ = 4.0 Hz, 1H; H^2), 8.18 (dd, $^3J_{(H,H)}$ = 8.0 Hz, $^4J_{(H,H)}$ = 4.0 Hz, 1H; H^3), 6.84 (d, $^3J_{(H,H)}$ = 8.0 Hz, 1H; H^4), 3.62 (t, $^3J_{(H,H)}$ = 8.0 Hz, 2H; =N-CH_2), 0.88 (t, $^3J_{(H,H)}$ = 8.0 Hz, 3H; CH_3), 1.55 (m, -CH_2 of methylene proton in side chain). IR (ν_{max}, cm^{-1}, KBr): 2920 ($\nu_{as(C-H)}$, CH_3), 2849 ($\nu_{s(C-H)}$, CH_3), 1656 ($\nu_{C=N}$), 1277 (ν_{C-O}).

[CdL_2]

Yield ~ 0.08g (74 %) Anal. Calc. (%) for $C_{50}H_{82}N_4O_6Cd$ (947.67): C, 63.31; H, 8.65; N, 5.91. Found: C, 63.33; H, 8.67; N, 5.87 %. FAB Mass: m/z = 948.5 (M^+-H). ^{1}H NMR (400 MHz, $CDCl_3$; Me_4Si at 25°C, ppm): δ = 8.30 (s, 1H; H^1), 8.24 (d, $^4J_{(H,H)}$ = 4.0 Hz, 1H; H^2), 8.19 (dd, $^3J_{(H,H)}$ = 8.0 Hz, $^4J_{(H,H)}$ = 4.0 Hz, 1H; H^3), 6.93 (d, $^3J_{(H,H)}$ = 8.0 Hz, 1H; H^4), 3.66 (t, $^3J_{(H,H)}$ = 8.0 Hz, 2H; =N-CH_2), 0.88 (t, $^3J_{(H,H)}$ = 8.0 Hz, 3H; CH_3), 1.71 (m, -CH_2 of methylene proton in side chain). IR (ν_{max}, cm^{-1}, KBr): 2919 ($\nu_{as(C-H)}$, CH_3), 2850 ($\nu_{s(C-H)}$, CH_3), 1639 ($\nu_{C=N}$), 1275 (ν_{C-O}).

[HgL_2]

Yield ~ 0.07g (67 %) Anal. Calc. (%) for $C_{50}H_{82}N_4O_6Hg$ (1035.85): C, 57.92; H, 7.91; N, 5.40. Found: C, 57.95; H, 7.93; N, 5.54%. FAB Mass: m/z = 1036.6 (M^+-H). ^{1}H NMR (400 MHz, $CDCl_3$; Me_4Si at 25°C, ppm): 8.30 (s, 1H; H^1), 8.24 (d, $^4J_{(H,H)}$ = 4.0 Hz, 1H; H^2), 8.18 (dd, $^3J_{(H,H)}$ = 8.0 Hz, $^4J_{(H,H)}$ = 4.0 Hz, 1H; H^3), 6.89(d, $^3J_{(H,H)}$ = 8.0 Hz, 1H; H^4), 3.66 (t, $^3J_{(H,H)}$ = 8.0 Hz, 2H; =N-CH_2), 0.88 (t, $^3J_{(H,H)}$ = 8.0 Hz, 3H; CH_3), 1.46 (m, -CH_2 of methylene proton in side chain). IR (ν_{max}, cm^{-1}, KBr): 2916 ($\nu_{as(C-H)}$, CH_3), 2848($\nu_{s(C-H)}$, CH_3), 1642 ($\nu_{C=N}$), 1273 (ν_{C-O}).

3.3. Results and discussion

3.3.1. Synthesis and structural assessment

The ligand was synthesized from the condensation of 5-nitrosalicylaldehyde and octadecylamine. The complexes were prepared by slow addition of methanolic solution of 1 equivalent of $M(OAc)_2.nH_2O$ (M = Zn, Cd; n = 2 or Hg; n = 0) to a methanolic solution of the ligand (2 equivalents) (**Scheme 3.1**). Structures were ascertained by elemental analysis, ^{1}H NMR, FT-IR, UV-Visible and FAB-Mass spectroscopy. The FAB-mass spectral data were in compliance with the calculated formula weights of the compounds. The IR spectra of the ligand exhibited broad band at ~3432cm^{-1} owing to the presence of phenolic-OH group. The C=N stretching vibration of the ligand was located at ~1672cm^{-1}. In the complexes, ν_{CN} vibrational stretching frequency was shifted to lower wave number ($\Delta\nu$~30cm^{-1}) and ν_{OH} mode was absent. This clearly suggests the co-ordination of azomethine nitrogen and phenolate oxygen to the metal in the complexes. ^{1}H NMR spectra of the ligand consisted of a singlet at 15ppm due to the phenolic-OH proton and another singlet at 8.31ppm due to the imine proton. A relatively small up-field shift (~ 0.01ppm) of the –N=CH proton and absence of the signal for the phenolate proton in the ^{1}H NMR spectra of the metal complexes further suggested coordination through the phenolate oxygen and the azomethine nitrogen atom of the ligand. DFT studies (*vide infra*) revealed the geometry of the complexes to be distorted tetrahedral. The computed metal-O/N bond lengths and the bond angles (*vide infra*) complied well with related crystallographically characterized non-mesomorphic tetrahedral zinc–Schiff base complex.[53]

3.3.2. Liquid crystalline properties

Polarizing optical microscopy and differential scanning calorimetry:

The phase behaviour of the compounds was studied by polarizing optical microscopy (POM), differential scanning calorimetry (DSC) and variable temperature powder-XRD techniques. The phase sequence, transition temperatures and associated enthalpies are summarized in **Table 3.1**. The ligand is non-mesomorphic, the greater conformational flexibility of the un-coordinated ligand molecule is believed to be one plausible reason for its non-mesomorphic character. On complexation, this flexibility is reduced which might

be responsible for induction of mesomorphism in zinc(II) and cadmium(II) complexes. The mercury(II) complex, however, decomposed at 270°C precluding any mesomorphic study. Upon cooling the sample from isotropic melt, the zinc(II) complex showed a 'platelet texture'(**Fig. 3.1**) at 127°C, typical of smectic E (or crystal E) phase.[54] The DSC profile (**Fig. 3.2**) showed four transitions in heating and two in the cooling cycle. The peaks below the melting point are believed to have arisen from crystal-to-crystal transition which could not be detected in POM study. In the case of cadmium(II) complex, a fibrous texture was observed (**Fig. 3.3**) upon cooling at 228°C. The DSC trace (**Fig. 3.4**) revealed two transitions each in the heating and cooling scan. In contrast to the zinc complex, interestingly the mesophase for the cadmium(II) complex was quite stable over a wide temperature range (231°C-88°C). The reversibility of the thermal behaviour of the zinc(II) and cadmium(II) complexes was established by DSC through repeated heating and cooling runs.

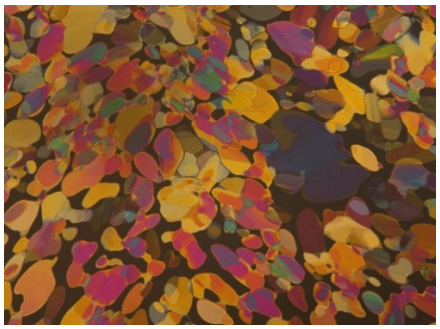

Fig. 3.1: Platelet texture of **[ZnL$_2$]** upon cooling at 127 °C.

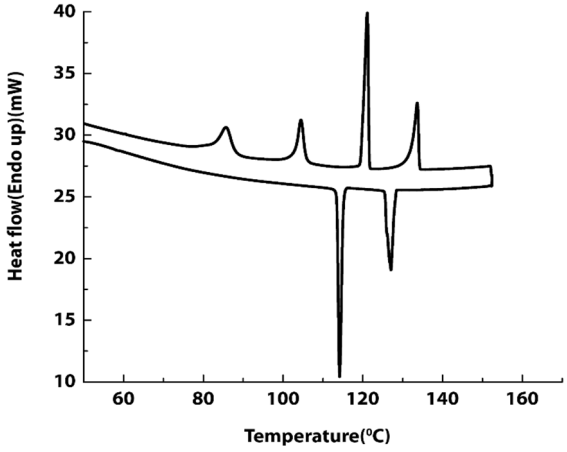

Fig. 3.2: DSC thermogram of **[ZnL$_2$]**.

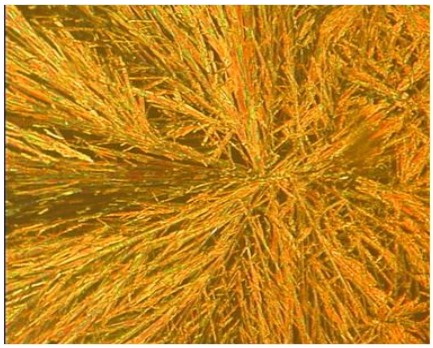

Fig. 3.3: Fibrous texture of **[CdL_2]** upon cooling at 228 °C.

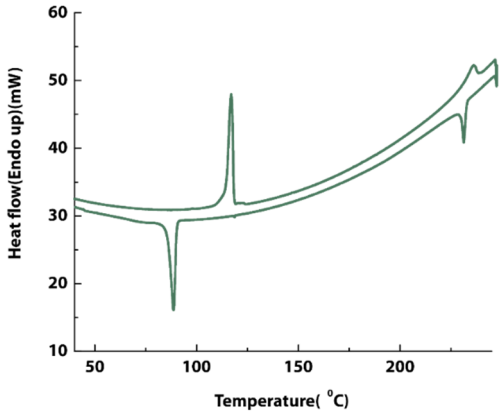

Fig. 3.4: DSC thermogram of **[CdL_2]**.

Table 3.1: Phase transition data of **[ZnL_2]** and **[CdL_2]**.

Compounds	**T (°C)[a]**	**Transition[b]**	**ΔH (kJ mol^{-1})**	**$\Delta_{trs}S$(J $K^{-1}mol^{-1}$)**
[ZnL_2]	85.7	Cr-Cr_1	16.9	47.1
	104.5	Cr_1-Cr_2	17.9	47.4
	121.1	Cr_2-SmE	36.9	93.6
	133.6	SmE-I	22.8	56.1
	127.1	I-SmE	25.2	62.9
	114.2	SmE-Cr_2	37.2	96.0
[CdL_2]	116.0	Cr- M_T	62.6	160.9
	235.8	M_T -I	15.4	30.2
	231.2	I- M_T	14.9	29.5
	88.6	M_T -Cr	47.4	131.0

[a] DSC peak temperature. [b]Cr: crystal, SmE: smectic E or soft crystal E, M_T = mesophase triclinic

Variable temperature PXRD study

The powder XRD profile of zinc(II) complexes, recorded at 122°C (**Fig. 3.5a**) consisted of one very sharp and three relatively weak reflections in the low angle region with a reciprocal spacing ratio of 1:2:3:4. The spacing could be assigned to (001), (002), (003) and (004) reflections of a lamellar lattice.[54,55] The (001) reflection is attributed to the smectic layer-spacing, *d*. Additionally, in the wide-angle region multiple harmonics corresponding to spacing of 5.0 Å (111) and 4.9 Å (200) were observed. Besides, a broad-scattering halo at ~ 4.6Å for the molten alkyl chains was observed. Presence of three strong reflections in the wide angle region indexed to the (111), (200) and (112) is a signature of SmE phase.[54,55] The phase was also validated by the characteristic 'platelet texture' observed in the POM study. The calamitic molecules thus, are presumed to be arranged in layers with orthorhombic symmetry and herringbone array, typical for a SmE phase (**Fig. 3.6**).[55] The aromatic core π-π interactions and hydrophobic interactions of the alkyl chains renders them to act as seggregated parts. The lattice parameters of the SmE phase are deduced as a = 9.89 Å, b = 6.05 Å, c = 24.65 Å and V_{cell} =1461.24Å^3 (**Table 3.2**). The calculated interlayer distance of 24.65 Å, is about half the length of the fully extended molecule as computed (*vide infra*) by DFT (42.1 Å). Molecular area for the proposed arrangement, A_M (65.38Å^2) is deduced from the relation $A_M = V_M/d$; (molecular volume, V_M = 1608.28 Å^3, density, ρ = 1 g/cm^3). Assuming a parallel arrangement of the molecules perpendicular to layer direction, the calculated A_M value would correspond to a cross-sectional area per aliphatic arm, $A_{ch} = A_M/2$ = 32.69Å^2 which is considerably larger than the cross-sectional area of a stretched molten alkyl arm (A_{ch} = 20.915 + 0.01593T = 22.85 Å^2 at 122°C). The alkyl arms are therefore believed to be considerably interdigitated within the layers.[5] The V_{cell} / V_M ratio (= 0.9) also suggests approximately one molecule per unit cell.

The diffractogram at 80°C (**Fig. 3.5b**) consisted of a number of sharp reflections in both the low as well as wide angles, consistent with the existence of a crystalline phase. Moreover, the diffractogram was devoid of any diffuse band at wide angles, thus pointing to the crystalline nature of the material.

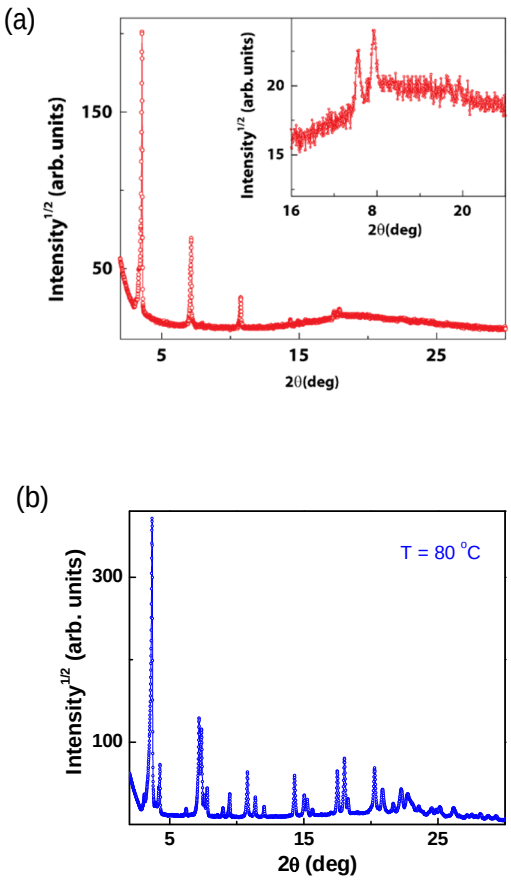

Fig. 3.5: PXRD pattern of **[ZnL$_2$]** recorded at (a) 122 °C and (b) at 80 °C.

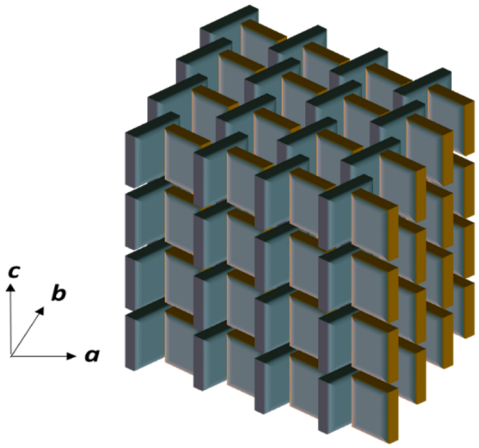

Fig. 3.6: The 'herringbone' model for the self-assembled rod-like complex molecules in smectic E phase. [G. W. Gray, J. W. G. Goodby, Smectic Liquid Crystal Texture and Structure; Leonard Hill: Glasgow, (1984); D. Demus, J. Goodby, G. W. Gray, H. W. Spiess, V. Vill, Handbook of Liquid Crystals, Wiley-VCH: Weinheim, Vol.2A (1998) pp.13.]

PXRD profile of cadmium(II) complex recorded at 210°C (**Fig. 3.7**) exhibited one very sharp and a number of relatively less intense reflections in the small angle region. The first and the fifth peak are indexed to (001) and (002) reflections, respectively, corresponding to a layered structure (**Table 3.2**). Other small and mid-angle reflections, however, indicated a three dimensional order of the mesophase. Besides, a poorly resolved diffuse halo at 4.6Å in the wide angle region indicated lateral short-range order of the molten alkyl chains. On the basis of these features, a highly ordered mesophase reminiscent of soft crystals has been suggested possessing both layer arrangement and 3D structure.[56-58] The observed pattern could be indexed to a primitive triclinic lattice (p_1) with lattice parameters a = 9.9Å, b = 21.7Å, c = 37.1Å; α = 47°, β = 68.6°, γ = 57° and V_{cell} = 4870Å^3. The mesophase with triclinic lattice may thus be designated as M_T.[57] The molecular volume, V_M =1462.45 Å^3 was calculated assuming a density close to 1.2 g/cm^3. Customarily, a density of 1 g/cm^3 is presumed for liquid crystalline mesophases resulting from organic molecules or metallomesogens incorporating lighter metals. On some instances a higher density values ($\rho \approx$ 1.1-1.2 g/cm^3) were reported for some smectic gold enriched dendrimers,[59] discotic gold pyrazolate compounds,[60] discotic cyclopalladated metallomesogens,[61] some potassium salts of crown ethers[62] and columnar hexaalkyloxytriphenylenes.[63] A higher density has thus been considered for the newly synthesized cadmium(II) complex considering a heavier metal core. Thus, approximately three molecules per unit cell in the triclinic lattice in the soft crystalline phase has been worked out.

Variation in the type of mesophase formed on changing the metal from zinc(II) to cadmium(II) and the lack of mesomorphism or thermal instability of the complex of the other congener, mercury(II) is not discernible at this moment. The noticeable aspect being the significant variation in the ionic radius of the metal center (Zn^{2+} = 0.74 Å; Cd^{2+} = 0.95 Å; Hg^{2+} =1.02 Å).[52,64]

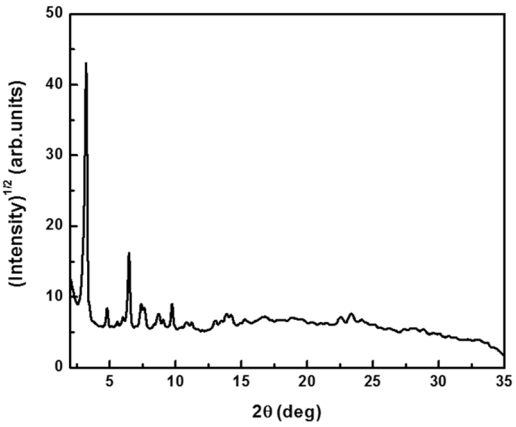

Fig. 3.7: PXRD profile of **[CdL_2]** at 210 °C.

Table 3.2: PXRD data of **[ZnL_2]** and **[CdL_2]**.

Compound	**Mesophase[a] Lattice constants/Å**	**$d_{obsd.}$/Å($d_{calcd.}$/Å)[b]**	**Miller indices *hkl*[c]**
[ZnL_2]	SmE(at 122°C) d = 24.65Å V_M = 1608.28Å^3 A_M = 65.38Å^2 a = 9.89 Å b = 6.05 Å c = 24.65 Å V_{cell} = 1461.24 Å^3	24.64(24.65) 12.33(12.32) 8.22(8.22) 6.17(6.16) 5.05(5.05) 4.95(4.95) 4.56^{diffuse}	(001) (002) (003) (004) (111) (200)
[CdL_2]	M_T (at 210°C) a = 9.9Å b = 21.7 Å c = 37.1 Å α = 47°, β = 68.6° γ = 57° V_{cell}= 4870Å^3 V_M=1462.45 Å^3	27.33(27.14) 18.37(18.05) 15.82(15.91) 14.64 (14.28) 13.65(13.57) 11.62(11.51) 10.15(10.29) 9.75(9.80) 9.08(9.08) 8.14(8.14) 6.80(6.80) 6.38(6.33) 6.22(6.24) 3.95(3.95) 3.80(3.80) 3.16(3.16) 4.56^{diffuse}	(0 0 1) (0 1 1) (0 1 2) (0 1 0) (0 0 2) (0 1 3) (0 1 -1) (1 1 1) (1 1 0) (1 1 3) (0 2 5) (1 -1 -1) (1 -1 -2) (1 -3 -3) (2 3 -1) (2 -2 -3)

[a] Molecular volume, V_M is calculated using the formula: $V_M = M/\lambda\rho N_A$, where M is the molecular weight of the compound, N_A is the Avogadro number, ρ is the density (~1g cm^{-3} for zinc(II) and 1.2 g cm^{-3} for cadmium(II) complex respectively), λ(T) is a temperature correction coefficient at the temperature of the experiment (T). $\lambda(T) = V_{CH2}(T^o) / V_{CH2}(T)$; where $V_{CH2}(T) = 26.5616 + 0.02023T$ is the volume of a methylene group (in $Å^3$) at a given temperature (in °C), and T° = 25 °C.

V_{cell}; unit cell volume: in the orthorhombic lattice, $V_{cell} = abc$; in triclinic lattice, $V_{cell} = abc\ (1 - cos^2\alpha - cos^2\beta - cos^2\gamma + 2cos\alpha\ cos\beta\ cos\gamma)^{1/2}$.

[b] d_{obsd} and d_{calcd} are the experimentally observed and calculated diffraction spacings, respectively. The distances are given in Å. [c] hkl are the Miller indices of the reflections in SmE and M_T phases, respectively.

3.3.3. Photophysical properties

The absorption spectra (**Fig. 3.8**) of the compounds were recorded in dichloromethane solution (10^{-5} M) at room temperature. The ligand showed three bands centered at 260nm, 323nm and 403nm, respectively, attributed to π-π* transition, localized on the aromatic rings and the C=N fragment (**Table 3.3**). Upon complexation, all the π-π* bands were virtually unaltered in the cadmium(II) and mercury(II) complexes. The absorption spectrum of the zinc(II) complex, however, exhibited only two bands at 257nm and 343nm. The low-intensity ligand centered π–π* transition peak at ~ 400nm observed in the spectra of ligand and complexes of cadmium(II) and mercury(II), appeared as a weak shoulder in the spectrum of zinc(II) complex while the second absorption peak was considerably bathochromically shifted (~33nm) compared to the free ligand. Photoluminescence studies of the compounds were carried out both in dichloromethane solution and in the solid state. The ligand is non-emissive, probable reason being the greater conformational flexibility. The complexes, however, exhibited fluorescence at room temperature with emission maxima at ~ 479nm. As a representative example, **Fig. 3.9** shows the photoluminescence spectra of cadmium(II) complex. The emission observed at room temperature in the complexes stem from the intra-ligand π-π* transition. Chelation provides rigidity to the ligand and reduces energy loss via non-radiative de-activation. The luminescence intensity of the complexes were found to decrease in the order: Zn > Cd > Hg. The emission quantum yields of the complexes have been determined in dichloromethane solution at room temperature and are found to be 0.20, 0.16 and 0.09, respectively for zinc, cadmium and mercury complexes. The lowest value of quantum yield for the mercury complex might be

due to the 'heavy atom' effect.[65] The solid state emission spectra of the complexes were recorded on a uniform thin film. The emission band of the complexes was quite broad and exhibited unusual blue shift (~ 467nm) compared to the solution while the emission intensity quenched largely. In solid state somewhat larger aggregation causes enhanced intermolecular interaction which explains the reduced luminescence intensity.[66] Further it has been argued that a tetrahedral geometry or formation of non-planar molecular shape as in the present case prevent inter-chromophoric contacts leading to blue shift of the emission maxima with respect to those observed for solution.[20]

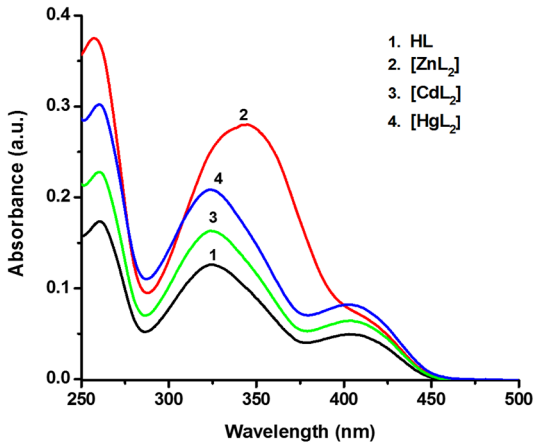

Fig. 3.8: UV-Visible spectra of the ligand and complexes (CH_2Cl_2; 10^{-5}M).

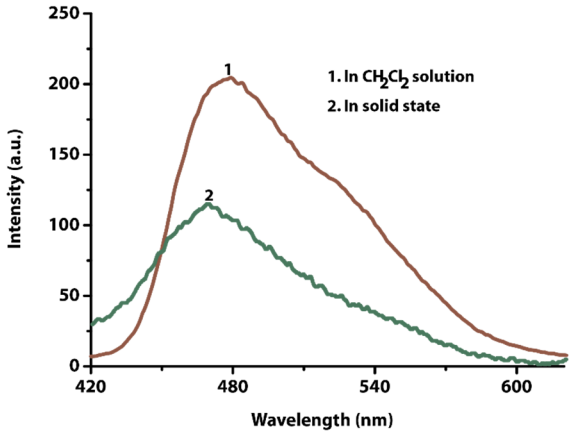

Fig. 3.9: Photoluminescence spectrum of **[CdL_2]** (10^{-5}M; $\lambda_{ex.}$ = 325nm).

Table 3.3: UV-visible and photoluminescence data of ligand and metal complexes.

Compounds	$\pi \rightarrow \pi^*$ (λ, nm; ε, l mol^{-1} cm^{-1})	[a]PL (λ, nm; Solution)	[a]PL (λ, nm; Solid)
HL	260 (17,464) 323 (12,689) 403(5,090)	-	-
$[ZnL_2]$	257 (37,547) 343 (28,107) 400*sh* (7,894)	475	470
$[CdL_2]$	259 (22,961) 324 (16,478) 400 (6,557)	479	467
$[HgL_2]$	259 (30,310) 322 (20,880) 399 (8,397)	470	466

[a]PL: Photoluminescence; *sh*: shoulder.

3.3.4. DFT Study

The density functional theory (DFT) calculations at the B3LYP level of theory on the ligand and its zinc(II), cadmium(II) and mercury(II) complexes were carried out using the GAUSSIAN 09 program.[67] The geometries of all species were fully optimized at the gradient corrected DFT level using three parameters fit of Becke's hybrid functional combined with the Lee-Yang-Parr correlation functional termed as B3LYP.[68,69] For zinc, cadmium and mercury atoms the Los Alamos effective core potential plus double zeta (LanL2DZ) basis set were employed[70] and the 6-311G(d,p) basis set was employed for all non-metal atoms. The gas phase ground state geometries of the ligand and its zinc, cadmium and mercury complexes were fully optimized using the restricted B3LYP methods without imposing any symmetry constraints. Calculations for vibrational frequencies were performed alongside each geometry optimization to ensure the stability of the ground state as denoted by the absence of imaginary frequencies. Natural bond

orbital (NBO) calculations were performed with the NBO code included in Gaussian 09 program at the same level of theory.[71]

Geometry optimization

DFT calculations were performed in order to get better insight into the electronic structure of the ligand as well as its complexes with zinc, cadmium and mercury. Optimized geometries of ligand, zinc, cadmium and mercury complexes (**Fig. 3.10a-d**) and computed significant geometric parameters of the complexes were evaluated at B3LYP level (**Table 3.4**), respectively. All metal (M = Zn, Cd, Hg) centers are tetra coordinated with two [N,O] donor bidentate ligands through two nitrogen atoms of two C=N groups and two oxygen atoms of two phenolic groups. The average M-O and M-N bond lengths in the complexes are 1.971 and 2.087, 2.159 and 2.290, and 2.266 and 2.357 Å, respectively (Table 4). The average O1–M–O2 bond angles are 128.4°, 135.8° and 139.3° and average N1–M–N2 bond angles are found to be 125.3°, 129.0° and 137.6°, respectively, around the zinc, cadmium and mercury atoms which deviate substantially from those expected for a square planar motif indicating a distorted tetrahedral geometry. The molecular length of zinc(II), cadmium(II) and mercury(II) complexes computed from DFT are found to be 42.1Å, 42.4 Å and 42.7 Å, respectively.

Natural bond orbital (NBO) analysis

DFT with natural bond orbital (NBO) analysis allows deeper insight into the nature of metal-ligand bonding. The natural charges and electronic configuration of the atoms of the complexes and free ligand evaluated by natural bond orbitals (NBO) analysis are summarized in **Table 3.5**. The calculated natural charges on the metal ions, zinc, cadmium and mercury are considerably lower than the formal charge, +2. The electronic population on p_x, p_y and p_z orbitals of zinc, cadmium and mercury atoms in their respective complexes are found to be (0.0990, 0.1133 and 0.1026), (0.0730, 0.0800 and 0.0700) and (0.0529, 0.0695 and 0.0640), respectively. However, d_{xy}, d_{zx}, d_{yz}, $d_{x^2-y^2}$ and d_{z^2} orbitals of zinc, cadmium and mercury atoms in their complexes are occupied by more than 1.99 e^-. Comparing the atomic charges in the free ligand and its complexes with zinc, cadmium and mercury, it can be suggested that the atomic charge re-distribution occured on all the atoms.

The calculated natural atomic charges on zinc, cadmium and mercury are found to be +1.405, +1.487 and +1.394, respectively, which reflects ligand-to-metal charge transfer in all the complexes. According to the NBO, the electronic configuration of Zn is: [core] $4s^{0.303}d^{9.974}p^{0.31}$, which corresponds to 18 core electrons, 10.27 valence electrons (on 4s and 3d atomic orbitals) and 0.31 Rydberg electrons (mainly on 4p orbital) giving 28.58 electrons. This is consistent with the calculated natural atomic charge on zinc atom (+1.405) in its complex. The electronic configuration of Cd is: [core]$5s^{0.30}4d^{9.985}p^{0.22}$, with 36 core electrons, 10.28 valence electrons (on 5s and 4d atomic orbitals) and 0.22 Rydberg electrons (mainly on 5p orbitals) leading to 46.50 electrons which matched well with the calculated natural charge on cadmium atom (+1.487) in the complex. The electronic configuration of mercury atom in its complex is calculated to be [core]$6s^{0.445}d^{9.976}p^{0.196}d^{0.01}$ that matches well with the calculated natural charge on mercury atom (+1.394) in the complex. The natural atomic charge on oxygen atoms of the ligand bound to metal ions change from -0.614 to -0.795 and -0.800 in zinc complex, to -0.807and -0.812 in cadmium complex and to -0.785 and -0.779 in mercury complex, respectively, while the atomic charges on nitrogen atom of the ligand changes from -0.433 to -0.634 and -0.629, to -0.637 and 0.633 and to -0.618 and -0.613 on complexation with zinc, cadmium and mercury, respectively (**Table 3.5**). The optimized geometry also revealed that the distance between oxygen and aromatic carbon (O-$C_{ar.}$) increases from 1.271 in free ligand to 1.314 Å, 1.318 Å and 1.286 Å in zinc, cadmium and mercury complexes, respectively. The O-$C_{ar.}$ bond is weakened upon complex formation implying coordination through oxygen.

Frontier molecular orbitals

Frontier molecular orbitals play an important role in determining the electronic properties of molecules.[72] The LUMO and HOMO energies of the free ligand and its complexes with zinc, cadmium and mercury are calculated to be -0.254eV and -1.816eV, -2.349eV and -6.520 eV, -2.568eV and -6.524eV and -2.244eV and-6.384eV, respectively. The corresponding energy differences (ΔE) are 1.562eV, 4.171eV, 3.956eV and 4.140eV, respectively. A small HOMO–LUMO gap implies a low kinetic stability and high chemical reactivity, because it is energetically favourable to add electrons to LUMO or to extract

electrons from a HOMO. The calculated HOMO–LUMO gap of the complexes revealed that the zinc complex is relatively more stable than the rest.

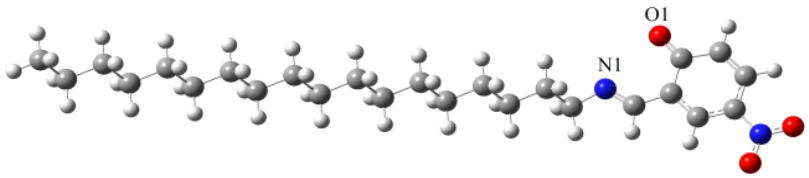

Fig. 3.10a: Optimized structure of the ligand, **HL**.

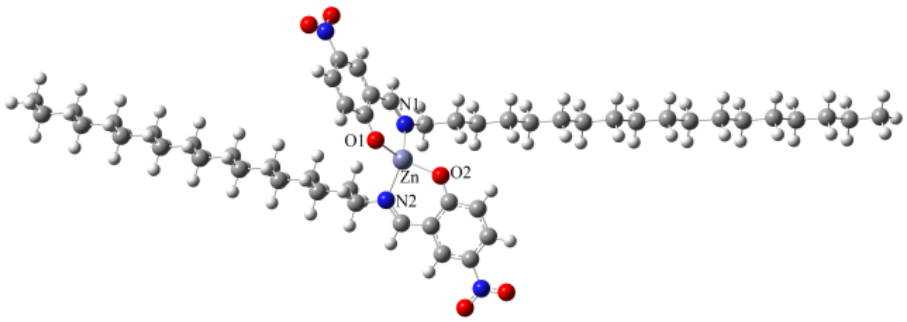

Fig. 3.10b: Optimized structure of **[ZnL$_2$]**.

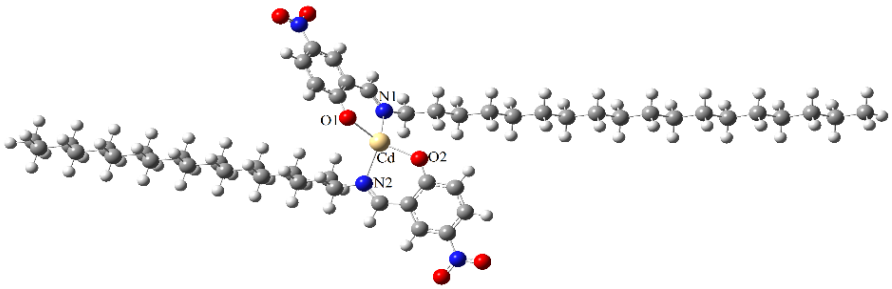

Fig. 3.10c: Optimized structure of **[CdL$_2$]**.

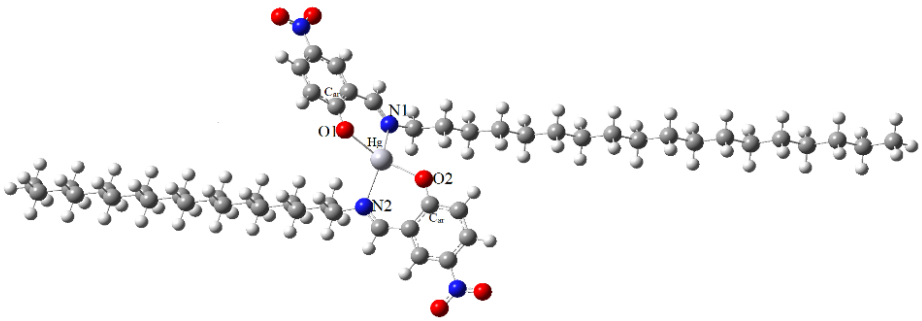

Fig. 3.10d: Optimized structure of **[HgL_2]**.

Table 3.4: Selected bond lengths (Å) and bond angles (°) for zinc(II), cadmium(II) and mercury(II) complexes evaluated at B3LYP level.

Structural parameters	Zn	Cd	Hg
M—O1	1.971	2.159	2.269
M—O2	1.971	2.158	2.263
M—N1	2.087	2.289	2.354
M—N2	2.088	2.291	2.361
O1—M—O2	128.4	135.8	139.3
N1—M—N2	125.3	129.0	137.6
O1—M—N1	93.0	86.2	83.7
O2—M—N2	92.8	86.0	83.5
O1—M—N2	108.6	111.8	108.7
O2—M—N1	112.1	114.4	113.8

Table 3.5: Natural atomic charges and natural electron configuration of selected atoms of the ligand and zinc(II), cadmium(II) and mercury(II) complexes evaluated at B3LYP level.

Atoms	**Ligand**		**Zn^{2+}**		**Cd^{2+}**		**Hg^{2+}**	
	Charge	Configuration	Charge	Configuration	Charge	Configuration	Charge	Configuration
O1	-0.614	[core]$2S^{1.72}2p^{4.89}$	-0.795	[core]$2S^{1.67}2p^{5.12}3p^{0.01}$	-0.807	[core]$2S^{1.68}2p^{5.12}3p^{0.01}$	-0.785	[core]$2S^{1.69}2p^{5.09}3p^{0.01}$
O2			-0.800	[core]$2S^{1.67}2p^{5.12}3p^{0.01}$	-0.812	[core]$2S^{1.68}2p^{5.12}3p^{0.01}$	-0.779	[core]$2S^{1.69}2p^{5.08}3p^{0.01}$
N1	-0.433	[core]$2S^{1.39}2p^{4.03}3p^{0.01}$	-0.634	[core]$2S^{1.35}2p^{4.26}3p^{0.01}$	-0.637	[core]$2S^{1.36}2p^{4.26}3p^{0.01}$	-0.613	[core]$2S^{1.36}2p^{4.24}3p^{0.01}$
N2			-0.629	[core]$2S^{1.35}2p^{4.26}3p^{0.01}$	-0.633	[core]$2S^{1.36}2p^{4.25}3p^{0.01}$	-0.68	[core]$2S^{1.36}2p^{4.24}3p^{0.01}$
M			1.405	[core]$4S^{0.30}3d^{9.97}4p^{0.31}$	1.487	[core]$5S^{0.30}4d^{9.98}5p^{0.22}$	1.394	[core]$5S^{0.44}5d^{9.97}6p^{0.19}6d^{0.01}$

3.4. Conclusion

A new N-alkylated bidentate [N,O]-donor rod shaped salicylaldimine Schiff base has been synthesized and complexation with Group 12, d^{10} -metal ions were achieved from an interaction of the Schiff base and Zn^{2+} or Cd^{2+} or Hg^{2+} ions. The ligand is neither fluorescent nor mesomorphic. However, the zinc(II) and cadmium(II) complexes besides being fluorescent showed highly ordered mesophase. The complexes exhibited luminescence both in solid and solution state. The mercury(II) complex though luminescent, decomposed prior to melting. DFT calculations carried out using GAUSSIAN 09 program at B3LYP level revealed a distorted tetrahedral geometry for all the complexes. Examples of tetrahedral coordination geometry exhibiting liquid crystallinity are rather uncommon. The application potential of the newly synthesised complexes as multi-functional material are avenues to be explored in near future.

REFERENCES

[1] J. Hanna, *Opto-Electron. Rev.*, 2005, **13**, 259.

[2] W. Z. Yuan, Z.-Q. Yu, P. Lu, C. Deng, J. W. Y. Lam, Z. Wang, E.-Q. Chen, Y. Mad, B. Z. Tang, *J. Mater. Chem.*, 2012, **22**, 3323 and references therein.

[3] F. Vera, J.L. Serrano, T. Sierra, *Chem. Soc. Rev.*, 2009, **38**, 781.

[4] A. Crispini, M. Ghedini, D. Pucci, *Beilstein J. Org. Chem.*, 2009, **5**, 1.

[5] H.A.R. Pramanik, G. Das, C.R. Bhattacharjee, P.C. Paul, P. Mondal, S. K. Prasad, D.S. S. Rao, *Chem. Eur. J.*, 2013, **19**, 13151.

[6] A. A. Knyazev, Y. G. Galyametdinov, B. Goderis, K. Driesen, K. Goossens, C. G. Walrand, K. Binnemans, T. Cardinaels, *Eur. J. Inorg. Chem*., 2008, 756.

[7] E. Tritto, R. Chico, G. Sanz-Enguita, C. L. Folcia, J. Ortega, S. Coco, P. Espinet, *Inorg. Chem.*, 2014, **53**, 3449.

[8] M. Micutz, M. Iliş, T. Staicu, F. Dumitraşcu, I. Pasuk, Y. Molard, T. Roisneld, V. Cîrcu, *Dalton Trans.*, 2014, **43**, 1151.

[9] M. Krikorian, S. Liu, T. M. Swager, *J. Am. Chem. Soc*., 2014, **136**, 2952.

[10] C. Cuerva, J. A. Campo, P. Ovejero, M. R. Torres, E. Oliveira, S. M. Santos, C. Lodeiro, M. Cano, *J. Mater. Chem. C*, 2014, **2**, 9167.

[11] A. M. Talarico, M. Ghedini, C. O. Rossi, E. I. Szerb, *Soft Matter*, 2012, **8**, 11661.

[12] A. Santoro, A. M. Prokhorov, V. N. Kozhevnikov, A. C. Whitwood, B. Donnio, J. A. G.Williams, D. W. Bruce, *J. Am. Chem. Soc.*, 2011, **133**, 5248.

[13] S. Debnath, H. F. Srour, B. Donnio, M. Fourmigué, F. Camerel, *RSC Adv*., 2012, **2**, 4453.

[14] C. R. Bhattacharjee, C. Datta, G. Das, R. Chakrabarty, P. Mondal, *Polyhedron*, 2012, **33**, 417.

[15] T. Cardinaels, J. Ramaekers, P. Nockemann, K. Driesen, K. Van Hecke, L. Van Meervelt, S. B. Lei, S. De Feyter, D. Guillon, B. Donnio, K. Binnemans, *Chem. Mater.*, 2008, **20**, 1278.

[16] S. Coco, C. Cordovilla, P. Espinet, J. Martin-Alvarez, P. Munoz, *Inorg. Chem*., 2006, 45, 10180.

[17] M. J. Mayoral, P. Ovejero, J. A. Campo, J. V. Heras, E. Pinilla, M. R. Torres, C. Lodeiro, M. Cano, *Dalton Trans.*, 2008, 6912.

[18] P. Ovejero, E. Asensio, J. V. Heras, J. A. Campo, M. Cano, M. R. Torres, C. Núñez, C. Lodeiro, *Dalton Trans.*, 2013, **42**, 2107.

[19] D. Pucci, A. Crispini, M. Ghedini, M. La Deda, P. F. Liguori, C. Pettinari, E. I. Szerb, *RSC Adv.*, 2012, **2**, 9071.

[20] E. Cavero, S. Uriel, P. Romero, J.L. Serrano, R. Giménez, *J. Am. Chem. Soc*., 2007, **129**, 11608.

[21] A. Kishimura, T. Yamashita, K. Yamaguchi, T. Aida, *Nat. Mater.*, 2005, **4**, 546.

[22] A. Barbieri, G. Accorsi, N. Armaroli, *Chem. Commun.*, 2008, 2185.

[23] R. C. Evans, P. Douglas, C. Winscom, *J. Coord. Chem. Rev.*, 2006, **250**, 2093.

[24] A. Kajal, S. Bala, S. Kamboj, N. Sharma, V. Saini, *J. Catal.*, 2013, 2013, http://dx. doi.org/10.1155/2013/893512. Article ID 893512.

[25] S. Kumar, D.N. Dhar, P.N. Saxena, *J. Sci. Ind. Res.*, 2009, **68**, 181.

[26] I. Kostova, L. Saso, *Curr. Med. Chem.*, 2013, **20**, 4609.

[27] Y. Xin, J. Yuan, *Polym. Chem.*, 2012, **3**, 3045.

[28] K. M. Abuamer, A. A. Maihub, M. M. El-Ajaily, A. M. Etorki, M. M. Abou-Krisha, M. A. Almagani, *Int. J. Org. Chem.*, 2014, **4**, 7.

[29] K. C. Gupta, A. K. Sutar, *Coord. Chem. Rev*., 2008, **252**, 1420.

[30] H. Xu, R. Chen, Q. Sun, W. Lai, Q. Su, W. Huang, X. Liu, *Chem. Soc. Rev.*, 2014, **43**, 3259.

[31] A. K. Neeraj, V. Kumar, R. Prajapati, S. K. Asthana, K. K. Upadhyaya, J. Zhao, *Dalton Trans.*, 2014, **43**, 5831.

[32] N. Hoshino, *Coord. Chem. Rev.*, 1998, **174**, 77.

[33] O. N. Kadkin, J. An, H. Han, Y. G. Galyametdinov, *Eur. J. Inorg. Chem.*, 2008, 1682.

[34] C. R. Bhattacharjee, C. Datta, G. Das, P. Mondal, *Liq. Cryst.*, 2012, **39**, 373.

[35] M. Marcos, A. Omenat, J. Barberá, F. Durán, J. L. Serrano, *J. Mater. Chem.*, 2004, **14**, 3321.

[36] K. Nejati, Z. Rezvani, *New J. Chem.*, 2003, **27**, 1665.

[37] Y. Galyametdinov, V. Ksenofontov, A. Prosvirin, I. Ovchinnikov, G. Ivanova, P. Gütlich, W. Haase, *Angew. Chem., Int. Ed.*, 2001, **40**, 4269.

[38] J. Barberá, E. Castel, R. Jiménez, M. Marcos, J. L. Serrano, *Mol. Cryst. Liq. Cryst.*, 2001, **362**, 89.

[39] C. R. Bhattacharjee, G. Das, P. Goswami, P. Mondal, S. K. Prasad, D.S. S. Rao, *Polyhedron*, 2011, **30**, 1040.

[40] D. Pucci, I. Aiello, A. Bellusci, A. Crispini, M. Ghedini, M. La Deda, *Eur. J. Inorg. Chem.*, 2009, 4274.

[41] P. A. Spegt, A. E. Skoulios, *Acta Crystallogr.*, 1963, **16**, 301.

[42] B. A. Gregg, M. A. Fox, A. J. Bard, *J. Am. Chem. Soc.*, 1989, **111**, 3024.

[43] S. A. Hudson, P. M. Maitlis, *Chem. Rev.*, 1993, **93**, 861.

[44] O. Celik, O. Dag, *Angew. Chem., Int. Ed.*, 2001, **40**, 3799.

[45] O. Dag, S. Alayoğlu, I. Uysal, *J. Phys. Chem. B*, 2004, **108**, 8439.

[46] F. Neve, O. Francescangeli, A. Crispini, *Inorg. Chim. Acta*, 2002, **338**, 51.

[47] E. Terazzi, J. -M. Benech, J. -P. Rivera, G. Bernardinelli, B. Donnio, D. Guillon, C. Piguet, Dalton Trans., 2003, 769.

[48] A. Pegenau, T. Hegmann, C. Tschierske, S. Diele, *Chem. Eur. J.*, 1999, **5**, 1643.

[49] C. Cuerva, P. Ovejero, J. A. Campo, M. Cano, *New J. Chem.*, 2014, **38**, 511.

[50] R. Giménez, A.B. Manrique, S. Uriel, J. Barberá, J. L. Serrano, *Chem. Commun.*, 2004, 2064.

[51] G. Barberio, A. Bellusci, A. Crispini, M. Ghedini, A. Golemme, P. Prus, D. Pucci, *Eur. J. Inorg. Chem.*, 2005, 181.

[52] F. Morale, R. L. Finn, S. R. Collinson, A. J. Blake, C. Wilson, D. W. Bruce, D. Guillon, B. Donnio, M. Schroder, *New J. Chem.*, 2008, **32**, 297.

[53] P. Shang, L. Zhang, *J. Chem.*, 2013, http://dx.doi.org/10.1155/2013/206847.

[54] S. M. Schultz, G. Kehr, R. Fröhlich, G. Erker, N. Kapernaum, C. Hägele, F. Giesselmann, S. Laschat, R. Judele, A. Baro, *Liq. Cryst.*, 2007, **34**, 919.

[55] S. Diele, S. Tosch, S. Mahnke, D. Dem, *Cryst. Res. Technol.*, 1991, **26**, 809.

[56] F. Lincker, B. Heinrich, R. De Bettignies, P. Rannou, J. Pecaut, B. Grevin, A. Pron, B. Donnio, R. Demadrille, *J. Mater. Chem.*, 2011, **21**, 5238.

[57] K. Oikawa, H. Monobe, K. Nakayama, T. Kimoto, K. Tsuchiya, B. Heinrich, D. Guillon, Y. Shimizu, M. Yokoyama, *Adv. Mater.*, 2007, **19**, 1864.

[58] B. G. Kim, S. Kim, J. Seo, N. -K. Oh, W. -C. Zin, S. Y. Park, *Chem. Commun.*, 2003, 2306.

[59] C. Cordovilla, S. Coco, P. Espinet, B. Donnio, *J. Am. Chem. Soc.*, 2010, **132**, 1424.

[60] J. Barberá, A. Elduque, R. Giménez, F. J. Lahoz, J. A. López, L. A. Oro, J. L. Serrano, *Inorg. Chem.*, 1998, **37**, 2960.

[61] A. Ionescu, N. Godbert, A. Crispini, R. Termine, A. Golemme, M. Ghedini, *J. Mater. Chem.*, 2012, **22**, 23617.

[62] M. Kaller, C. Deck, A. Meister, G. Hause, A. Baro, S. Laschat, *Chem.-Eur. J.*, 2010, **16**, 6326.

[63] V. A. Gunyakov, N. P. Shestakov, S. M. Shibli, *Liq. Cryst.*, 2003, **30**, 871.

[64] J. D. Lee, *Concise Inorganic Chemistry, fifth ed., Wiley, India*, 2007. pp. 839.

[65] Y. -W. Dong, R. -Q. Fan, P. Wang, L. -G. Wei, X. -M. Wang, H. -J. Zhang, S. Gao, Y. -L. Yang, Y. -L. Wang, *Dalton Trans.*, 2015, **44**, 5306.

[66] T. Yu, W. Su, W. Li, Z. Hong, R. Hua, B. Li, *Thin Solid Films*, 2007, **515**, 4080.

[67] M. J. Frisch, G. W. Trucks, H. B. Schlegel, G. E. Scuseria, M. A. Robb, J. R. Cheeseman, G. Scalmani, V. Barone, B. Mennucci, G. A. Petersson, H. Nakatsuji, M. Caricato, X. Li, H. P. Hratchian, A. F. Izmaylov, J. Bloino, G. Zheng, J. L. Sonnenberg, M. Hada, M. Ehara, K. Toyota, R. Fukuda, J. Hasegawa, M. Ishida, T. Nakajima, Y.Honda, O. Kitao, H. Nakai, T. Vreven, J. A. Montgomery Jr., J. E. Peralta, F. Ogliaro, M. Bearpark, J. J. Heyd, E. Brothers, K. N. Kudin, V. N. Staroverov, R. Kobayashi, J. Normand, K. Raghavachari, A. Rendell, J. C. Burant, S. S. Iyengar, J. Tomasi, M. Cossi, N. Rega, J. M. Millam, M. Klene, J. E. Knox, J. B. Cross, V. Bakken, C. Adamo, J. Jaramillo, R. Gomperts, R. E. Stratmann, O. Yazyev, A. J. Austin, R. Cammi, C. Pomelli, J. W. Ochterski, R. L. Martin, K. Morokuma, V. G. Zakrzewski, G. A. Voth, P. Salvador, J. J. Dannenberg, S. Dapprich, A. D. Daniels, Ö. Farkas, J. B. Foresman, J.V. Ortiz, J. Cioslowski, D. J. Fox, GAUSSIAN 09, Gaussian Inc., Wallingford CT, 2009.

[68] A. D. Becke, *J. Chem. Phys.*, 1993, **98**, 5648.

[69] C. Lee, W. Yang, R. G. Parr, *Phys. Rev. B*, 1988, **37**, 785.

[70] P. J. Hay, W. R. Wadt, *J. Chem. Phys.*, 1985, **82**, 270.

[71] J. N. Harvey, *Annu. Rep. Prog. Chem. Sect. C.: Phys. Chem.*, 2006, **102**, 203.

[72] I. Fleming, *Frontier Orbitals and Organic Chemical Reactions*, *Wiley*, *London*, 1976.